doi:10.1016/j.jmb.2007.06.061 J. Mol. Biol. (2007) 372, 619–632

JMB

Available online at www.sciencedirect.com

ScienceDirect

ELSEVIER

TFIIA Changes the Conformation of the DNA in TBP/TATA Complexes and Increases their Kinetic Stability

Aaron R. Hieb[1], Wayne A. Halsey[2], Meredith D. Betterton[3] Thomas T. Perkins[2,4], Jennifer F. Kugel[1] and James A. Goodrich[1]*

[1]*Department of Chemistry and Biochemistry, University of Colorado at Boulder, 215 UCB Boulder, CO 80309-0215, USA*

[2]*JILA and National Institute of Standard and Technology University of Colorado at Boulder, 440 UCB, Boulder CO 80309-0440, USA*

[3]*Department of Physics University of Colorado at Boulder, 390 UCB, Boulder CO 80309-0390, USA*

[4]*Department of Molecular Cellular, Developmental Biology University of Colorado at Boulder, 347 UCB, Boulder CO 80309-0347, USA*

**Corresponding author*

Eukaryotic mRNA transcription by RNA polymerase II is a highly regulated complex reaction involving numerous proteins. In order to control tissue and promoter specific gene expression, transcription factors must work in concert with each other and with the promoter DNA to form the proper architecture to activate the gene of interest. The TATA binding protein (TBP) binds to TATA boxes in core promoters and bends the TATA DNA. We have used quantitative solution fluorescence resonance energy transfer (FRET) and gel-based FRET (gelFRET) to determine the effect of TFIIA on the conformation of the DNA in TBP/TATA complexes and on the kinetic stability of these complexes. Our results indicate that human TFIIA decreases the angle to which human TBP bends consensus TATA DNA from 104° to 80° when calculated using a two-kink model. The kinetic stability of TBP/TATA complexes was greatly reduced by increasing the KCl concentration from 50 mM to 140 mM, which is more physiologically relevant. TFIIA significantly enhanced the kinetic stability of TBP/TATA complexes, thereby attenuating the effect of higher salt concentrations. We also found that TBP bent non-consensus TATA DNA to a lesser degree than consensus TATA DNA and complexes between TBP and a non-consensus TATA box were kinetically unstable even at 50 mM KCl. Interestingly, TFIIA increased the calculated bend angle and kinetic stability of complexes on a non-consensus TATA box, making them similar to those on a consensus TATA box. Our data show that TFIIA induces a conformational change within the TBP/TATA complex that enhances its stability under both *in vitro* and physiological salt conditions. Furthermore, we present a refined model for the effect that TFIIA has on DNA conformation that takes into account potential changes in bend angle as well as twist angle.

Keywords: TATA binding protein (TBP); TFIIA; fluorescence resonance energy transfer (FRET); DNA bending; transcription

Introduction

The TATA binding protein (TBP) is a central component of the eukaryotic mRNA transcription machinery. TBP binding to TATA boxes in promoter DNA is thought to be the initial event for general transcription factor recruitment at many promoters.[1–3] The binding of TBP to TATA DNA has been well characterized functionally and structurally, and the complex is considered to form with high affinity and kinetic stability. TBP binds in the minor groove of DNA and bends the DNA.[4–7]

Present address: A. R. Hieb, German Cancer Research Center, Division of Biophysics of Macromolecules, Heidelberg, Germany.

Abbreviations used: FRET, fluorescence resonance energy transfer; TBP, TATA binding protein; gelFRET, gel-based FRET; TAF, TBP associated factor.

E-mail address of the corresponding author: james.goodrich@colorado.edu

Crystal structures of TBP bound to TATA DNA have shown that the C-terminal DNA binding domain of TBP looks like a saddle with stirrups hanging from each end.[8–11] Each stirrup contains phenylalanine residues, which insert into the minor groove on each side of a 6 bp stretch of DNA, centered in the middle of the 8 bp TATA box. Insertion of the phenylalanine residues disrupts the base stacking interactions and allows TBP to bend the DNA.[8–11] TBP causes minor grove widening and changes the roll, rise, and twist of the TATA DNA.

The affinity with which TBP binds the DNA is dictated by the conformational flexibility of the DNA, and not by sequence specific interactions.[8,12–16] Therefore, flexible TATA sequences and sequences biased to bend toward the major groove are preferred for binding, whereas rigid GC-rich sequences and sequences biased to bend toward the minor groove are not. Fluorescence resonance energy transfer (FRET) studies by Parkhurst and colleagues have shown that yeast TBP bends DNA 80° whereas human TBP bends the DNA 102° in solution, as determined using a two-kink model in which the net bend angle from linear is the sum of the two equal bend angles at each kink.[17–19] The bend angles calculated from these studies are thought to be the average between the bent and unbent populations, rather than one static bend angle. Therefore, at saturating TBP concentrations, the average calculated bend angle is dictated by the equilibrium constant for bending/unbending. FRET studies coupled with Monte-Carlo simulations on multiple TBP bound DNA sequences have also shown that sequence changes within the DNA can alter the average DNA bend angle, and larger bend angles are generally correlated with an increase in transcriptional activity.[13,19,20]

The binding of yeast and archaeal TBP to TATA DNA are sensitive to cation concentration, where decreases in both affinity and rate of association have been observed with increased salt concentration.[21–23] This effect is thought to be in part due to a hydrating water at the protein–DNA interface and accessibility of cations within the binding pocket.[13,21–23] It has also been suggested that weaker recognition sequences allow for more rapid exchange of ions into the hydrophobic binding pocket of TBP, making them more sensitive to salt concentration.

The affinity and stability of TBP bound to DNA is enhanced by transcription factor TFIIA.[24–26] Human TFIIA is a three-subunit protein totaling 69 kDa and is believed to be required for transcription at most eukaryotic promoters.[27–30] It has been shown to interact with multiple activators, TBP associated factors (TAFs), and general transcription factors, including TBP.[3] Studies of TFIIA/TBP/TATA ternary complexes show that TFIIA contacts TBP as well as the DNA upstream and within the TATA box.[31–36]

With the goal of obtaining a better understanding of the roles that TBP and TFIIA play in transcriptional regulation, we used FRET assays to accurately measure changes in the distance between the ends of the DNA upon binding TBP and TBP/TFIIA. We found that TFIIA enhances the stability of the bent state of TBP/TATA complexes, makes the complexes less sensitive to salt concentration, and causes the conformation of non-consensus TATA DNA bound by TBP to be the same as that of a consensus TATA box. We also developed a refined model for visualizing the effect of TFIIA on TATA DNA conformation, which evaluates potential changes in bend angle and twist.

Results

FRET can be used to determine the architecture of macromolecular complexes by measuring intermolecular distances between various components. FRET has been used to study the bending of DNA by yeast and human TBP.[17,18] To begin to assess the effect of other transcription factors on the TBP-induced DNA bend, we established FRET assays. We initially probed TBP binding to the TATA-14 construct shown in Figure 1(a). This 14 bp construct contains donor (Alexa-555) and acceptor (Alexa-647) fluorophores attached to the 3′ ends of opposite strands. Fluorescence emission data was collected on the TATA-14 construct (Figure 1(b)), which displays a mild degree of FRET in the absence of TBP (continuous line). Addition of human TBP (broken line) decreased the donor signal and enhanced the acceptor signal, consistent with closer proximity of the donor–acceptor pair and increased FRET.

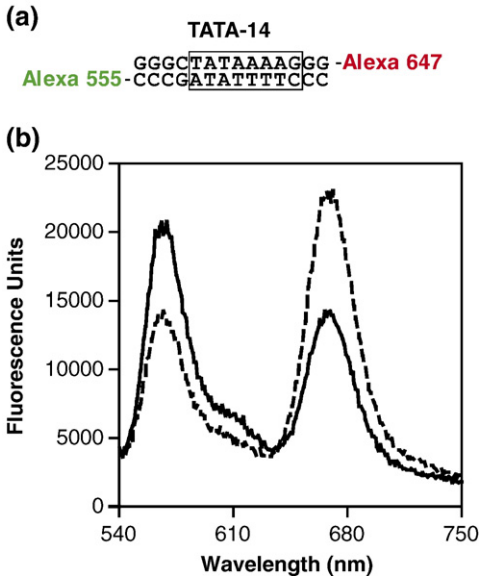

Figure 1. The use of FRET to monitor the bending of TATA DNA by human TBP. (a) Diagram of the 14 bp TATA-14 DNA. Alexa-555 (donor) and Alexa-647 (acceptor) are attached to the 3′ ends of the DNA. (b) TBP changes DNA conformation causing increased FRET. Shown are the emission spectra of unbound TATA-14 (continuous line) and TBP bound TATA-14 (broken line) excited at 532 nm.

To facilitate rapid study of TBP induced DNA bending, we performed FRET studies on samples in parallel using a 384 well borosilicate microplate and measuring the fluorescence with a Typhoon fluorimager. Preliminary studies showed that this system allowed us to accurately measure distance changes in the TATA-14 DNA probe at concentrations and sample volumes as low as 1 nM and 20 μl, respectively. Figure 2(a) shows the donor (green), FRET (red), and the pseudo-color overlay of the FRET and donor signals. As the TBP concentration increased, a shift toward FRET was observed. Figure 2(b) shows a plot of average FRET efficiency (determined using the equations shown in Materials and Methods) *versus* TBP concentration. As the concentration of TBP increased, the average end-to-end distance of the TATA-14 DNA decreased and eventually reached a plateau, indicating the DNA was saturated with TBP. From this plateau point, we calculated the average end-to-end distance of TATA-14 when bound by TBP to be 43 Å. Using this distance measurement and a modified version of the previously published two-kink model[19] (Figure 2(c)), we calculated an average DNA bend angle (α) of 104°. This value is in agreement with the bend angle of 102° that Parkhurst and colleagues determined for human TBP bound to a TATA box of the same sequence.[18]

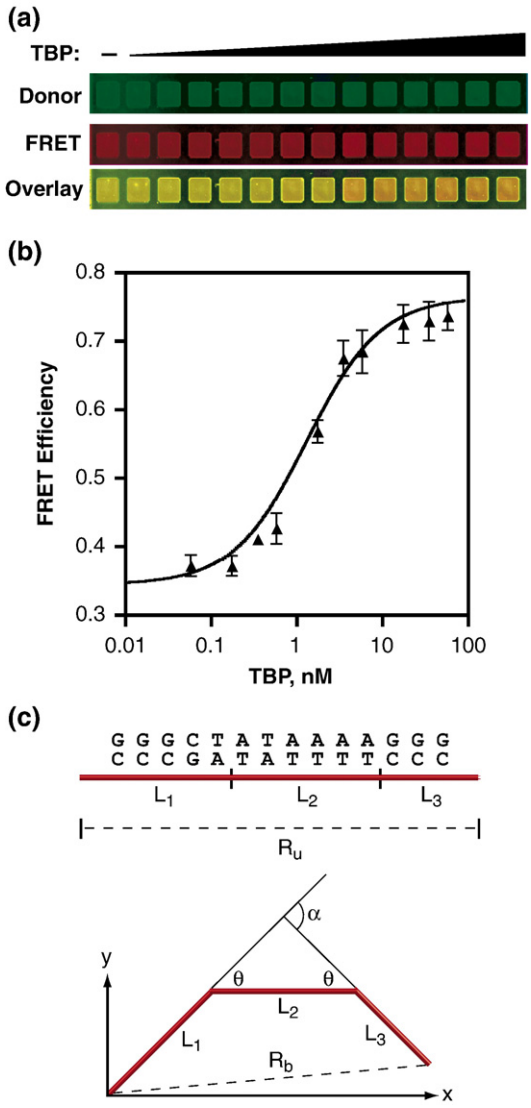

Figure 2. A two-kink model used to evaluate the bending of DNA by TBP. (a) FRET increases as TBP is titrated into reactions containing TATA-14. TBP was titrated from 0.08 nM to 60 nM using 1 nM TATA-14. Reactions were analyzed in a 384 well borosilicate microplate using a Typhoon fluorimager. Donor (green), FRET (red), and the pseudo-color overlay of the FRET and donor signals are shown. (b) FRET efficiency increases due to an increase in the concentration of TBP. FRET efficiency was calculated at each concentration of TBP. Data points are the average of three experiments and error bars represent one standard deviation. (c) Two-kink bend model used to calculate the angle (α) to which TBP bends TATA DNA.[19] The DNA is shown as a red rod consisting of three segments with lengths (L_1, L_2, and L_3). The upper panel shows linear DNA and the sequence of the DNA construct. R_u is the measured end-to-end length of the unbound DNA. The lower panel shows bent DNA. R_b is the measured end-to-end length of the bound DNA.

Human TFIIA changes the conformation of the DNA in the TBP/TATA complex

We next asked whether the association of the general transcription factor TFIIA with the TBP/TATA-14 complex alters the conformation of the TATA DNA. Solution-based FRET assays were performed on the TATA-14 construct with saturating concentrations of human TBP (25 nM) and human TFIIA (50 nM). Although TFIIA binds to TBP in a 1:1 complex, TFIIA was added in a twofold molar excess over TBP to push the reaction toward TBP/TFIIA/TATA complexes. Figure 3(a) shows donor (green), FRET (red), and the pseudo-color overlay of the FRET and donor signals for unbound (wells 1–4), TBP bound (wells 5–8), and TBP/TFIIA bound (wells 9–12) TATA-14. Visually, an increase in FRET signal can be observed in both TBP/TATA-14 and TBP/TFIIA/TATA-14 complexes compared to unbound TATA-14. When quantitated, the end-to-end distance for the TBP/TATA-14 complex was calculated to be 43 Å, whereas the end-to-end distance for the TBP/TFIIA/TATA-14 complex was 48.7 Å. Thus, TFIIA increased the average end-to-end distance by nearly 6 Å. The calculated two-kink bend angle for TBP bound complexes accordingly decreased from 104° to 80° upon association of TFIIA. When we added TFIIA to TATA-14 in the absence of TBP it did not cause a change in FRET (data not shown). Hence, TFIIA alone does not interact with the DNA in a manner that alters its conformation.

As a control to ensure that the FRET changes observed were not due to environmental effects on the fluorophores, we switched the positions of the donor and acceptor fluorophores to create the TATA-14* DNA. Figure 3(b) shows donor (green), FRET (red), and the pseudo-color overlay of the FRET and donor signals for unbound (wells 1–4), TBP bound (wells 5–8), and TBP/TFIIA bound (wells 9–12)

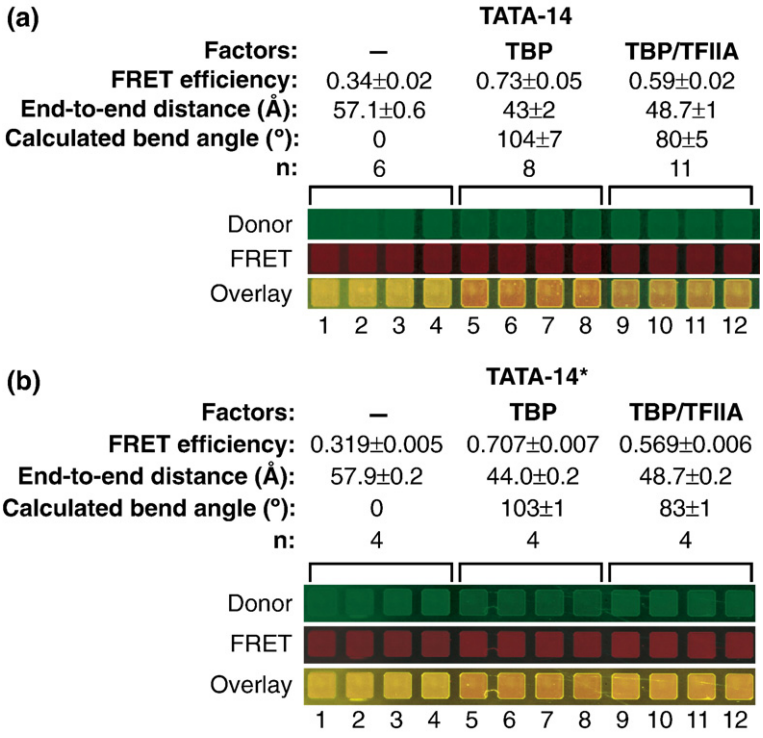

Figure 3. TFIIA decreases the angle to which TBP bends consensus TATA DNA. (a) Donor (green), FRET (red), and the pseudo-color overlay of the FRET and donor signals are shown for unbound (wells 1–4), TBP bound (wells 5–8), and TBP/TFIIA bound (wells 9–12) TATA-14. The average FRET efficiency, end-to-end distance, and calculated bend angle are shown along with the number of reactions performed (*n*) for each of the three conditions. Errors represent one standard deviation. (b) The calculated angle to which TBP bends the DNA is not affected by switching the positions of the fluorophores. The conditions were the same as in (a), with the exception that the TATA-14* DNA was used.

TATA-14*. The bend angles calculated for TBP/TATA-14* and TBP/TFIIA/TATA-14* complexes were 103° and 83°, respectively, consistent with the values obtained with the TATA-14 DNA. We conclude that the TFIIA-induced change in FRET is not due to environmental changes in the fluorophores, because the probability of the fluorophores experiencing identical environments at both of the 3′ ends of the DNA is highly unlikely.

These solution studies showed a change in end-to-end distance upon association of TFIIA; however, we could not elucidate whether this change was due to a change in DNA conformation, a shift in the equilibrium state between bound and free DNA, or a combination of the two. To distinguish between the two possibilities, we used gelFRET,[37] which allowed us to resolve TBP/TFIIA/TATA-14 complexes from partially formed complexes and unbound DNA. Binding assays for gelFRET experiments were assembled as they were for solution experiments, and samples were resolved by native polyacrylamide gel electrophoresis in salt conditions similar to those present in solution. After complexes were resolved from free DNA, the gels were imaged on a Typhoon fluorimager, quantitated, and FRET efficiency was determined as described in Materials and Methods. Figure 4(a) shows pseudo-color overlays of donor (green) and FRET (red) signals for lanes from a native gel containing TATA-14 and TATA-14* unbound and bound with TBP and TFIIA. The bend angles calculated for TATA-14 and TATA-14* in the bound bands were 83° and 87.8° respectively. Although these values are 3° to 5° greater than the bend angles calculated from solution studies, they are significantly lower than the bend angles calculated for the complexes lacking TFIIA. TBP/TATA complexes are generally not stable during native gel electrophoresis, however, we were able to detect weak TBP/TATA-14 and TBP/TATA-14* bands in gels. FRET measurements on these complexes yielded calculated bend angles of approximately 102° (data not shown). We therefore conclude that the change in bend angle upon addition of TFIIA to TBP/TATA complexes is caused by a change in the conformation of the bound DNA as opposed to a shift in equilibrium between bound and unbound species.

To determine whether protein binding in the native gel influenced the fluorescence intensity of either the donor or acceptor fluorophore, we performed controls in which ^{32}P was added to a 5′ end of the two TATA DNAs shown in Figure 4(b). Using DNAs that were both fluorescently and radioactively labeled allowed us to normalize for the amount of DNA present in unbound and bound species and calculate the ratio of fluorescence to radioactivity for the DNA in these complexes. If this ratio remained constant for both the donor and the acceptor fluorophores, then we could conclude that protein binding under gel conditions does not affect the fluorophores. The two ^{32}P-labeled DNAs were incubated with TBP and TFIIA and complexes were resolved using native gel electrophoresis. Gels were first scanned for fluorescence using donor settings for the donor labeled construct and acceptor settings for the donor–acceptor construct. Gels were then dried and subject to phosphorimagery. Figure 4(b) shows representative donor (green), acceptor (red), and radioactivity (grey) data. The ratios of fluorescence to radioactivity did not change between unbound and TBP/TFIIA bound bands for either the donor or acceptor fluorophores, indicating that

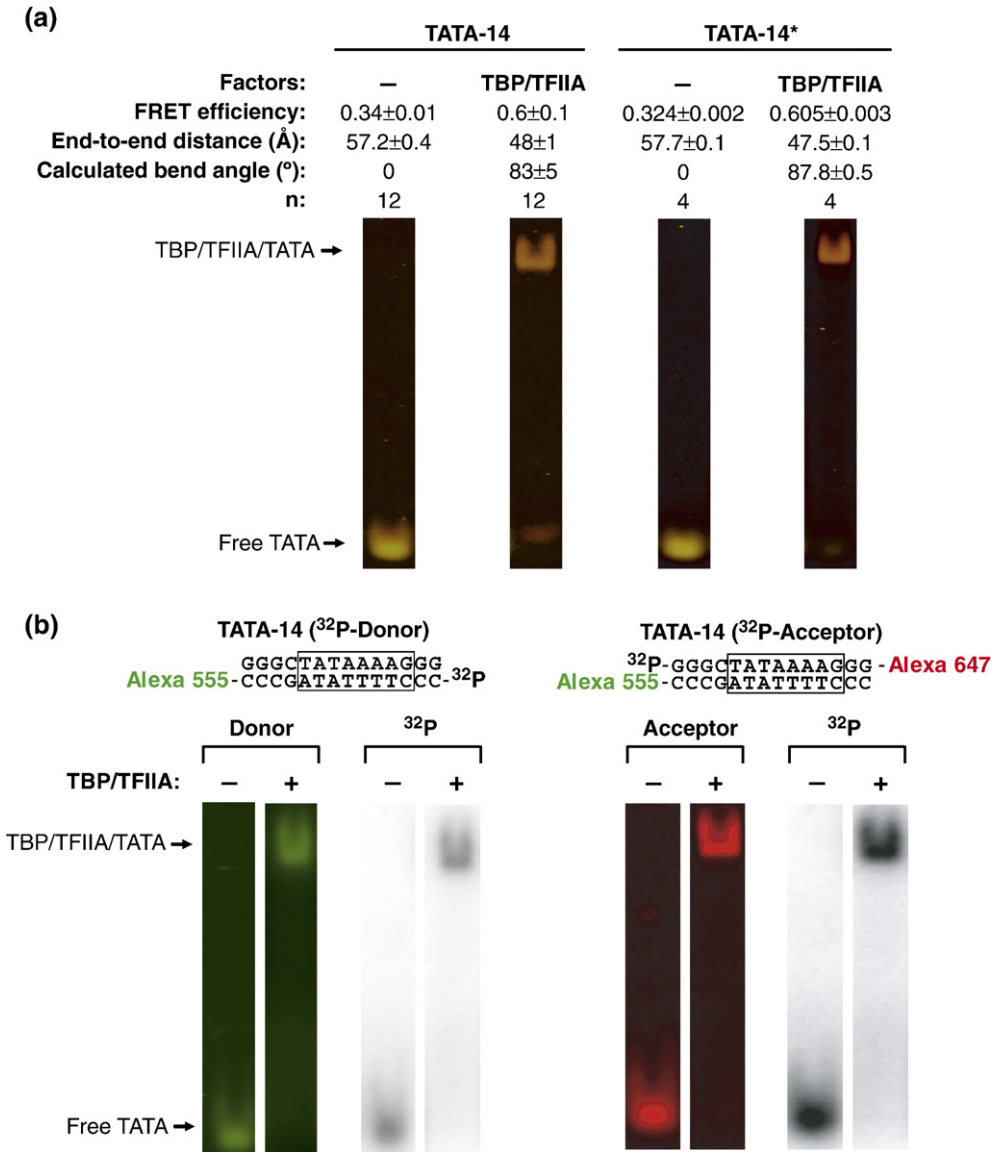

Figure 4. The decrease in the end-to-end distance of the TATA DNA observed in the presence of TFIIA is due to a change in the conformation of the DNA. (a) gelFRET was used to measure the end-to-end distance of TATA-14 and TATA-14* DNA in the presence and absence of TBP and TFIIA. After resolving unbound and bound DNA on a native gel, fluorescence was imaged using a Typhoon fluorimager. Shown are overlays of donor (green) and FRET (red) signals for lanes from a representative gel. The average FRET efficiency, end-to-end distance, and calculated bend angle are shown along with the number of reactions analyzed (*n*) for each of the four conditions. Errors represent one standard deviation. (b) ^{32}P-labeling was used to determine the effect of protein binding in native gels on the fluorescence intensities of the donor and acceptor fluorophores. Constructs used in gelFRET to determine quantum yield changes for donor and acceptor fluorophores when bound by TBP and TFIIA are shown at the top. The lanes show the donor (green), acceptor (red), and radioactive (grey) signals for unbound and TBP/TFIIA bound DNAs.

protein binding did not substantially affected the fluorophore intensities.

TFIIA stabilizes TBP/TATA complexes

Since TFIIA altered the conformation of the TBP/TATA complex, we questioned whether TFIIA would also affect the kinetic stability of this complex, perhaps by "locking" the TBP/TATA complex into a more stable state. We first determined dissociation rate constants for TBP/TATA-14 complexes and the TBP/TFIIA/TATA-14 complexes under our standard *in vitro* binding and transcription conditions (50 mM KCl, 4 mM $MgCl_2$). After allowing complexes to form, excess unlabeled TATA-14 DNA was added and the FRET efficiency was measured over time using a fluorimeter. Figure 5(a) shows a plot of relative FRET efficiency *versus* time for TBP/TATA-14 (blue squares) and TBP/TFIIA/TATA-14 (green triangles). Data were fit to an equation for single exponential decay. Under our standard *in vitro* conditions, TFIIA decreased the dissociation rate

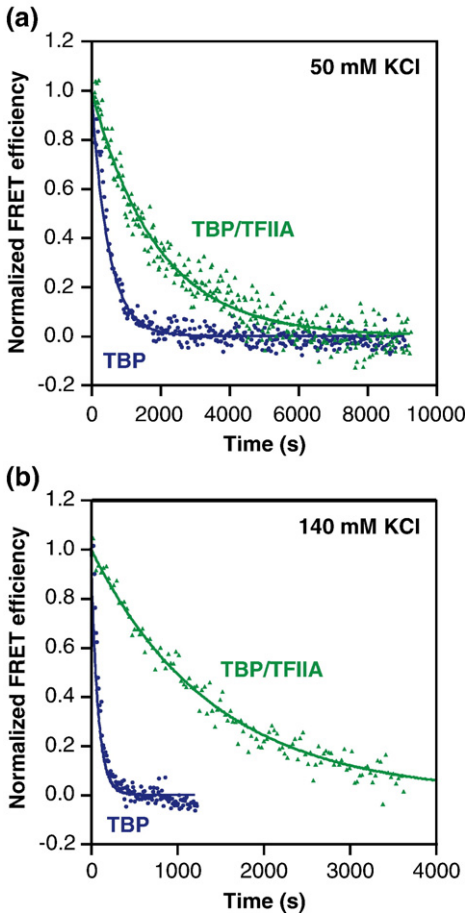

Figure 5. TFIIA increases the kinetic stability of the TBP/TATA complex. (a) Rates of dissociation were measured under our standard monovalent salt concentration (50 mM KCl) for TBP/TATA-14 and TBP/TFIIA/TATA-14 complexes. The change in FRET over time after adding excess unlabeled TATA-14 DNA was measured and data were fit to a single exponential decay rate. The rate constants for dissociation were 2.1×10^{-3} s^{-1} and 5.3×10^{-4} s^{-1} for TBP/TATA-14 (blue squares) and TBP/TFIIA/TATA-14 (green triangles), respectively. (b) Measured rates of dissociation under physiological monovalent salt concentration (140 mM KCl) for TBP/TATA-14 and TBP/TFIIA/TATA-14 complexes. The change in FRET over time after adding excess unlabelled TATA-14 DNA was measured and data were fit to a single exponential decay rate. The rate constants for dissociation were 1.3×10^{-2} s^{-1} and 7.1×10^{-4} s^{-1} for TBP/TATA-14 (blue squares) and TBP/TFIIA/TATA-14 (green triangles), respectively.

constant from 2.1×10^{-3} s^{-1} to 5.3×10^{-4} s^{-1}. Thus, TFIIA caused a fourfold stabilization of the TBP/TATA complex.

It was important to determine how TBP/TATA stability is affected by TFIIA under physiological salt conditions, because it is known that the TBP/DNA complex is sensitive to the monovalent salt concentration[21,22] and the physiological salt concentration in a cell is much greater than that typically used for *in vitro* binding and transcription assays such as those we have used here. An experiment comparable to that shown in Figure 5(a) was performed at salt concentrations more similar to those found in human cells (140 mM KCl, 5 mM $MgCl_2$, 5 mM NaCl) and yielded dissociation rate constants of 1.3×10^{-2} s^{-1} for TBP/TATA-14 (Figure 5(b), blue squares) and 7.1×10^{-4} s^{-1} for TBP/TFIIA/TATA-14 (Figure 5(b), green circles). The increased salt concentration caused a sixfold increase in the dissociation rate constant for TBP/TATA-14 complexes, but only a 1.4-fold increase in the dissociation rate constant for TBP/TFIIA/TATA-14 complexes. Thus, under physiological salt concentrations, TBP does not bind DNA stably and TFIIA causes a substantial increase in the kinetic stability of the TBP/TATA complex (18-fold). This is consistent with a model in which TFIIA induces a conformational change in the TBP/TATA complex that "locks" TBP on DNA, thereby attenuating the destabilizing effect of higher monovalent salt concentrations on the TBP/TATA-14 complex.

TFIIA induces a stabilizing conformation in complexes on a mutant TATA box

We have shown that TFIIA induces both a conformational change upon TBP bound DNA and stabilizes TBP binding to a strong TATA box. We next asked whether TFIIA would behave similarly when TBP is bound to a weaker TATA box, differing from the consensus TATA sequence. Figure 6(a) shows the sequence of TATA(A3)-14, a non-consensus TATA DNA in which the T:A (non-template strand:template strand) base-pair at position three of the TATA box was changed to an A:T base-pair. This non-consensus TATA box has been shown to have significantly reduced TBP binding affinity and transcriptional activity.[7,38–40] Solution binding assays were performed and a pseudo-color overlay of donor (green) and FRET (red) signals is shown in Figure 6(b). The calculated bend angles for the TATA (A3)-14 DNA bound by TBP and TBP/TFIIA were 71° and 87°, respectively. TBP alone appeared to bend the TATA(A3)-14 DNA far less (33°) than it bent the consensus TATA-14 DNA. In the presence of TFIIA, however, the TATA(A3)-14 DNA was bent to a similar degree as the TATA-14 DNA (87° and 80°, respectively). We also performed gelFRET experiments on the TBP/TFIIA/TATA(A3)-14 complex. The pseudo-color overlay of donor (green) and FRET (red) signals from gelFRET is shown for free TATA(A3)-14 DNA and TBP/TFIIA/TATA(A3) complexes in Figure 6(c). The bend angle calculated for the complex was 81.5°.

Dissociation rate constants were determined for TBP/TATA(A3)-14 and TBP/TFIIA/TATA(A3)-14 complexes under our standard *in vitro* binding conditions (50 mM KCl). Representative data are shown in Figure 6(d). TBP/TATA(A3)-14 complexes dissociated rapidly with a dissociation rate constant of 6.0×10^{-2} s^{-1}. TFIIA caused a 55-fold stabilization of these complexes; TBP/TFIIA/TATA(A3)-14 complexes had a dissociation rate constant of 1.1×10^{-3} s^{-1}. We also found that increasing the

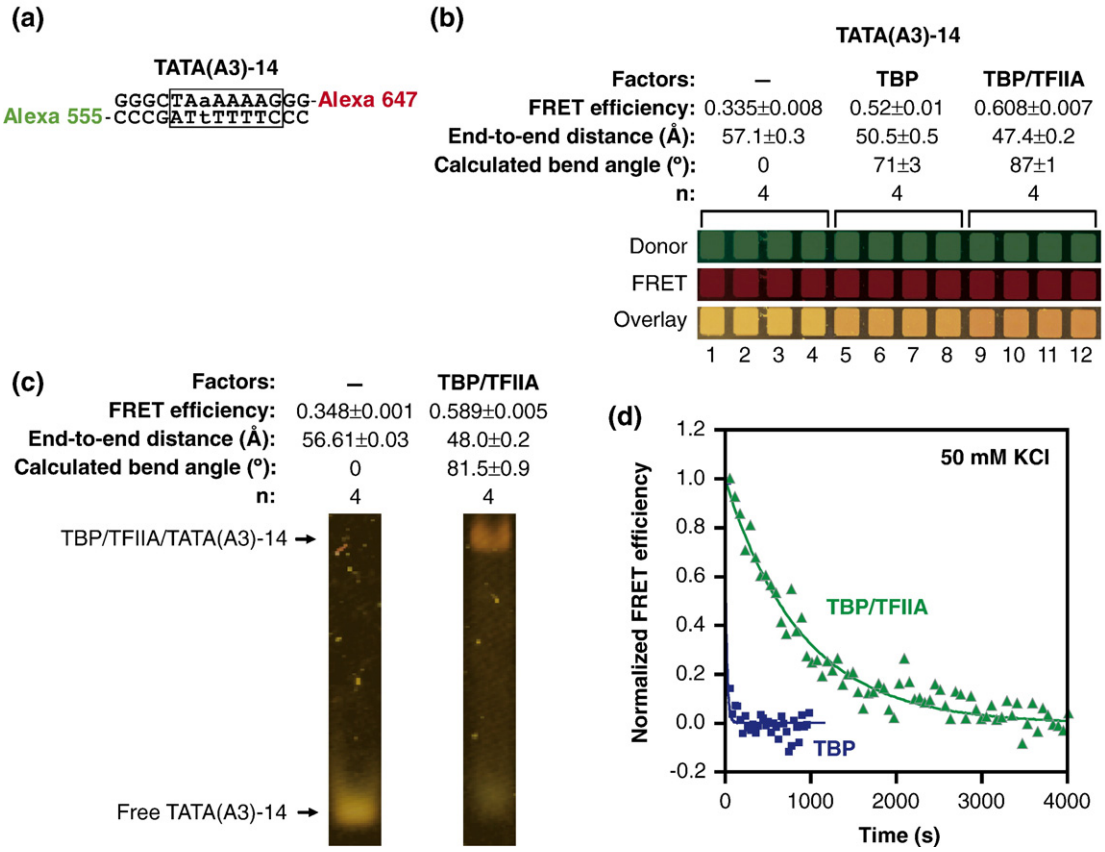

Figure 6. TFIIA increases the kinetic stability with which TBP binds and the calculated angle to which TBP bends a non-consensus TATA DNA. (a) The mutant TATA(A3)-14 DNA contains a T/A base-pair in place of the A/T base-pair at the third position of the TATA box (lower case letters). (b) Solution FRET was used to measure the effects of TBP and TFIIA on the conformation of the TATA(A3)-14 DNA. Donor (green), FRET (red), and the pseudo-color overlay of the FRET and donor signals are shown for unbound (wells 1–4), TBP bound (wells 5–8), and TBP/TFIIA bound (wells 9–12) TATA(A3)-14. The average FRET efficiency, end-to-end distance, and calculated bend angle are shown along with the number of reactions performed (*n*) for each of the three conditions. Errors represent one standard deviation. (c) gelFRET was used to measure the effects of TBP and TFIIA on the conformation of the TATA(A3)-14 DNA. Unbound and TBP/TFIA bound TATA(A3)-14 DNA were resolved on a native gel and fluorescence was imaged using a Typhoon fluorimager. Shown are overlays of donor (green) and FRET (red) signals for lanes from a representative gel. The average FRET efficiency, end-to-end distance, and calculated bend angle are shown along with the number of reactions analyzed (*n*) for each of the two conditions. Errors represent one standard deviation. (d) TFIIA increased the kinetic stability of the TBP/TATA(A3)-14 complex. Rates of dissociation were measured under our standard monovalent salt concentration (50 mM KCl) for TBP/TATA(A3)-14 and TBP/TFIIA/TATA(A3)-14 complexes. The rate constants for dissociation were 6.0×10^{-2} s^{-1} and 1.1×10^{-3} s^{-1} for TBP/TATA(A3)-14 (blue squares) and TBP/TFIIA/TATA(A3)-14 (green triangles), respectively.

monovalent salt concentration to physiological conditions did not significantly affect the rate of dissociation of TBP/TFIIA/TATA(A3)-14 complexes (data not shown). These data are consistent with a model in which TFIIA causes a conformational change in TBP/TATA complexes at weak TATA boxes, resulting in enhanced kinetic stability and an increased tolerance of higher monovalent salt concentrations.

Discussion

Using quantitative FRET, we found that TFIIA changes the conformation of the DNA in TBP/TATA complexes. TBP alone induced a 104° bend in a consensus TATA DNA, as calculated using a two-kink bend model. TFIIA decreased the calculated bend angle to 80°. Native gel electrophoresis was used to isolate TBP/TFIIA/TATA complexes, and quantitative FRET on these complexes showed the effect of TFIIA was due to a change in the conformation of the TATA DNA in the complex, as opposed to a change in the fraction of complexes in the bound state at equilibrium. TBP bent a non-consensus TATA DNA less than the consensus TATA DNA in the absence of TFIIA; however, in the presence of TFIIA, the bend in non-consensus and consensus TATA DNA was similar. The kinetic stability of TBP/TATA complexes was found to be highly affected by monovalent salt concentration; under physiological conditions TBP bound DNA

transiently. Association of TFIIA greatly enhanced the kinetic stability of TBP bound to either a consensus or a non-consensus TATA sequence. These studies lead to a model in which TFIIA locks the TBP/TATA complex into a conformation that is kinetically stable at physiological salt concentrations on both consensus and non-consensus TATA sequences.

TBP binding and bending of TATA DNA as measured by quantitative FRET

Understanding the mechanism by which TBP binds DNA is important for understanding transcriptional regulation, as this binding event is an early step in recruitment of the general transcription factors to many promoters. In order to view DNA conformational changes upon binding of TBP and TFIIA, we used two methods for quantitative FRET involving controls for changes in both spectral overlap and fluorescence intensity upon protein binding. FRET assays were performed in a 384 well microplate, which allowed us to use small volumes and amounts of protein for steady-state visualization. Using this approach, we confirmed earlier results, which showed that human TBP bends the TATA DNA by 102° when evaluated with the two-kink bend model.[18] It is interesting to note that yeast TBP bends TATA DNA by 80°,[41] which is significantly less than that for human TBP, indicating that human TBP and yeast TBP have different properties in binding and bending TATA DNA.

The TBP/TATA complex has been found to be kinetically stable *in vitro* and was therefore thought to be stable in cells as well. Our studies show that although human TBP is bound stably to TATA DNA under standard *in vitro* transcription conditions ($k_{off} = 2.1 \times 10^{-3}$ s^{-1} at 50 mM KCl), TBP/TATA complexes are significantly less stable at salt concentrations more similar to those inside cells ($k_{off} = 1.3 \times 10^{-2}$ s^{-1} at 140 mM KCl). This sixfold increase in the rate constant for dissociation of human TBP/TATA complexes is larger than would have been predicted from previous studies of yeast TBP.[21] Increased monovalent salt has been shown to reduce both the association rate constant and the overall binding affinity of yeast TBP to DNA[21]; however, rate constants for dissociation were not directly measured. Using the affinity and association rate constants to calculate the dissociation rate constants indicates that changing the KCl concentration from 50 mM to 140 mM would result in only a 1.6-fold increase in the dissociation rate constant for yeast TBP/TATA complexes. An explanation for the apparent increased sensitivity of human TBP/TATA complexes to monovalent salt awaits further study.

Non-consensus TATA boxes have been shown to have reduced binding affinity for TBP and transcriptional activity relative to a consensus TATA box.[38,40,42] This deficiency correlates with a smaller average bend angle upon binding of yeast TBP and a shift toward the unbent state.[19] Our FRET data for human TBP binding to TATA(A3)-14 led to a calculated average bend angle of 71°, which is 33° less than that observed when human TBP binds the consensus TATA-14 under the same conditions. We also found that complexes between human TBP and the TATA(A3) mutant have much lower kinetic stability than complexes containing the consensus TATA box. This lower stability could result from a decrease in the time the complex spends in the bent state and/or the time TBP spends bound to the DNA, either of which would dramatically decrease transcriptional activity.

TFIIA alters the conformation of TBP bound TATA DNA and increases the kinetic stability of TBP/TATA complexes

While the conformation of the DNA in the TBP/TATA complex has been well characterized, the influence of additional transcription factors on TATA DNA architecture is less well understood. Using solution FRET and the two-kink bend model, we found that the angle at which TATA DNA is bent by human TBP changes from 104° to 80° upon the association of TFIIA. Using gelFRET, we found that DNA in a complex with TBP and TFIIA was bent 83°. The similarity between the solution FRET and gelFRET measurements allowed us to conclude that the change in FRET observed in the presence of TFIIA was due to a change in the conformation of the DNA, as opposed to a change in the fraction of DNA bound. The change in DNA conformation induced by TFIIA could result from interactions of TFIIA with TBP, the DNA, or both. Crystal structures have previously shown little deviation between DNA conformations when TBP is bound to TATA DNA alone or in the presence of TFIIA[31,35,36]; however, these complexes contained only the C-terminal DNA binding domain of TBP and portions of the TFIIA subunits. It is possible that protein–protein and/or protein–DNA interactions missing in these complexes contribute to the change in DNA conformation we observed with FRET when we used full-length human proteins. TFIIA could also cause additional changes in DNA conformation on longer TATA DNA constructs that allow more extensive TFIIA-DNA contacts.[34] We also note the calculated bend angle for the human TBP/TFIIA/TATA complex is identical to that measured for the yeast TBP/TATA complex without TFIIA.[17] It will be interesting to determine the effect of yeast TFIIA on DNA conformation in the yeast TBP/TATA complex.

Solution FRET and gelFRET indicated that TFIIA forces the TATA DNA into the same conformation for both a weak and a strong TATA box even though TBP alone bends these two DNAs differently. Specifically, the binding of TBP and TFIIA induced bends of approximately 80° in both the consensus TATA-14 DNA and the non-consensus TATA(A3)-14 DNA, whereas binding by TBP alone induced bends of 103° and 70° in these DNAs, respectively. This indicates that when TFIIA interacts with TBP/TATA, the resulting complex contains DNA in a

specific conformation regardless of the TATA sequence and its binding affinity for TBP.

We also found that human TFIIA enhances the kinetic stability of TBP/TATA complexes, and that the effect of TFIIA is very dramatic at physiological salt concentrations and with a non-consensus TATA box. The effect of TFIIA on the stability of TBP/TATA complexes was anticipated from the previous work of Pugh and colleagues, who found that human TFIIA increased the stability of TBP/TATA complexes by tenfold.[25] The most profound effect that we observed was the 55-fold kinetic stabilization of complexes formed on the non-consensus TATA(A3) DNA. Our work shows that TFIIA not only stabilizes TBP/TATA complexes, but also leads us to propose a model in which TFIIA locks the TATA DNA into a uniform bent state regardless of the salt concentration or the sequence of the TATA box. It is possible that this effect of TFIIA results from its ability to induce a conformational change in TBP that reduces the occupancy or accessibility of salt or water in the binding pocket between TBP and the DNA. Alternatively, the contacts TFIIA makes with the DNA may tether TBP to DNA if it releases its direct contacts, allowing TBP to rapidly rebind before completely dissociating.

Our studies provide both structural and functional insight into how TBP and TFIIA are involved in transcriptional regulation in cells. The transient nature by which TBP binds DNA under cellular salt conditions suggests that TBP alone will not be stably bound at promoters in cells, but instead may require other factors such as TFIIA and TAFs to stabilize the interaction. The rapid association and dissociation of TBP alone with DNA may be vital for the control of transcription. The recruitment of TFIIA to specific promoters may serve as a means to selectively increase TBP occupancy and hence transcription of genes that need to be actively transcribed under specific cellular conditions. Moreover, TFIIA might be critical for inducing a specific DNA conformation in TATA-less promoters, which may be an important aspect of setting levels of transcription from genes that lack TATA boxes.

A model for assessing the conformation of TATA DNA that considers bend and twist

The two-kink model, which has been used to calculate the bend angle of TATA DNA in complexes with TBP, assumes the bent DNA is planar.[19] It is likely that TBP also twists the DNA at one or both of the kinks, which would contribute to the overall change in end-to-end distance observed in our FRET experiments. Twist is apparent in Figure 7(a), which shows the crystal structure of human TBP from two views rotated 90° with respect to one another with extra DNA projected from the published structure to help observe the DNA trajectory.[8,11] The DNA is not planar, but extends into a third dimension as a result of twist induced by TBP. The crystal structure of the human TBP/TATA complex showed that TBP twists the DNA such that the angle between the incoming and outgoing DNA is 110°.[11]

To envision how twist would affect the DNA end-to-end distance, we created a two-kink-twist model that allows for twist in the right kink (Figure 7(b)). The model is characterized by two angles: the bend angle α and the twist angle γ. Segments 1 and 2 in the DNA construct are anchored in the *xy* plane indicated in light green. When γ is 0°, segment 3 is also in this plane, and the planar two-kink model can be used to calculate α. As γ changes from 0° through 360°, segment 3 will sweep out of this plane tracing a cone. The end of segment 3 will always be in the *yz* plane indicated in light blue. We have used the two-kink-twist model to aid in our understanding of the possible mechanism by which TFIIA alters the DNA in the TBP/TATA complex. Figure 7(c) shows possible combinations of bend and twist angles that could give rise to the distances we observed for TBP/TATA-14 (43 Å, blue curve) and TBP/TFIIA/TATA-14 (48.7 Å, green curve) complexes using solution FRET. As can be seen for both complexes, as the twist angle increases from 0° to 180°, the bend angle must also increase to maintain a constant end-to-end distance in our model. This analysis demonstrates that the end-to-end distance change caused by TFIIA can be accounted for by a change in the twist angle alone; the range of bend angles where this is possible is between the horizontal broken lines. According to our simple model, the increase in end-to-end distance upon association of TFIIA could result from decreased bend only, increased twist only, or a combination of bend and twist changes. The two extreme modes of changing the end-to-end distance have different energetic implications for TFIIA binding. If TFIIA decreases the TATA DNA bend angle, strain within the DNA would be reduced. Alternatively, if TFIIA increases the TATA DNA twist angle, torsion would be added to the system, resulting in increased strain within the DNA.

The possibility that the change in end-to-end distance we observed here could be caused by changes in both bend and twist raises interesting questions about the effect of TFIIA on transcription. TFIIA could alter both distance and phasing of the TATA box with respect to the transcriptional start site. By altering these parameters, the binding and activity of other transcription factors may be affected positively or negatively. Therefore, the conformation of the TBP/TFIIA/TATA complex may be tunable and play a vital role in rapid responses to gene regulation.

Materials and Methods

DNA constructs and proteins

Recombinant human TBP and TFIIA were prepared as described.[43] Oligonucleotides containing a primary amine attached to the 3′ end *via* a six-carbon linker (Integrated DNA Technologies) were phenol/chloroform extracted,

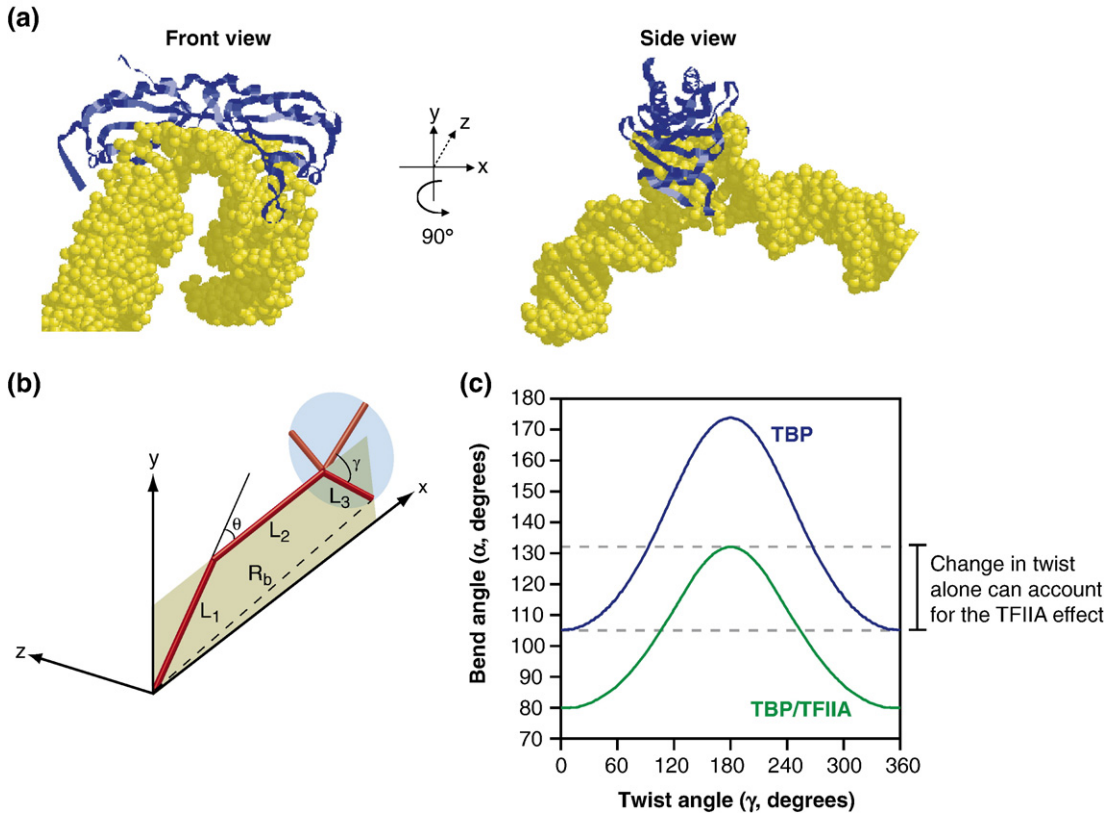

Figure 7. A model for TBP binding that includes both bend and twist. (a) A two-kink bend and a twist in TATA DNA is induced by human TBP. Two views of the human TBP/TATA crystal structure are shown, with additional DNA added to each end of the TATA box used in the structural studies.[11] (b) A two-kink-twist model for the DNA in TBP/TATA complexes. The planar two-kink bend model[19] was used as the basis for incorporating a twist into a third dimension. See the text for a description of the model. (c) TFIIA induced conformational changes in TBP/TATA complexes could arise from changes in bend angle, twist angle, or combinations of bend and twist angles. Plotted are the bend and twist angle combinations that could give rise to the end-to-end distances observed for the TBP/TATA-14 (blue curve) or TBP/TFIIA/TATA-14 (green curve) complexes based on the two-kink-twist model. The broken lines represent the region where changes in twist only could result in the observed end-to-end distance change caused by TFIIA.

ethanol precipitated, and dissolved in water at a concentration of 4 mM. Oligonucleotide solution (4 μl) was added to 41 μl of 0.1 M sodium borate (pH 8.5). Alexa-555 (donor) or Alexa-647 (acceptor) (100 μg, containing a succinimidyl ester; Molecular Probes) was dissolved in 7 μl of dimethyl sulfoxide (DMSO). The oligonucleotide and dye were mixed and agitated overnight in the dark. The fluorescently labeled oligonucleotide was purified using a G-25 spin column followed by chromatography on a C18 column (Supelco; 25 cm×4.6 mm) using 0.1 M triethylammonium acetate and an acetonitrile gradient (10%–20% (v/v)). Fractions containing labeled oligonucleotide were dried, pooled, and resuspended in TE (10 mM Tris (pH7.0), 0.1 mM EDTA). TATA DNAs were generated by annealing two complementary oligonucleotides (heating to 95 °C for 2 min, then slow cooling to room temperature). Annealing reactions were performed with a mild excess of acceptor labeled DNA relative to donor labeled DNA to ensure all donor-labeled DNA had a paired acceptor DNA strand.

Binding reactions and solution FRET measurements

Unless stated otherwise, binding reactions were performed using *in vitro* transcription reaction conditions.[44] Briefly, proteins were preincubated at 30 °C for 3 min in 10 μl of buffer A containing 20% (v/v) glycerol, 20 mM Tris (pH 7.9), 100 mM KCl, 1 mM DTT, and 50 μg/ml bovine serum albumin (BSA). DNA (2 nM) was preincubated at 30 °C for 3 min in 10 μl of buffer B containing 20 mM Hepes (pH 7.9), 8 mM $MgCl_2$, and 1 mM DTT. The solutions containing proteins and DNA were combined and incubated at 30 °C for 20 min, followed by addition of poly[dG-dC]-poly[dG-dC] (GE Healthsciences) to a final concentration of 25 μg/ml. Eighteen μl of each reaction were then added to individual wells of a 384 well borosilicate microplate (Intermountain Scientific Corporation) and scanned for fluorescence using a Typhoon Imager (GE biosciences). Scanning was performed with laser and filter settings adjusted for the excitation and emission wavelengths specified at a focal point 3 mm from the surface and light emission collected with a PMT set at 600 V. Fluorescence was quantitated with ImageQuant® software.

gelFRET experiments

Binding reactions were assembled as described above using 1.5-5 nM TBP and 5-50 nM TFIIA. Where indicated, TATA DNA was ^{32}P-labeled at the 5′ end using [γ-^{32}P]ATP

with T4 polynucleotide kinase. Gels were composed of 4% (w/v) acrylamide (37.5:1), 5% glycerol, 0.5X Tris-borate-EDTA, 4 mM magnesium acetate, and 50 mM potassium acetate. After addition of poly[dG-dC]-poly [dG-dC], reactions were incubated for 2 min and loaded onto a running gel. Gels were run at 150 V for 1-2 h at 4 °C. Gels were kept between the borosilicate plates (C.B.S. Scientific) and scanned for fluorescence using a Typhoon fluorimager (GE biosciences). Scanning was performed as described above. For experiments including radioactivity, gels were dried and analyzed by phosphorimagery. Fluorescence and radioactivity in bands were quantitated with ImageQuant® software.

FRET calculations

The FRET efficiency (E) from donor to acceptor is related to the distance between them (R) by the following equation:[45]

$$E = R_0^6/(R_0^6 + R^6)$$

The FRET pair used here (AlexaFluor-555 (D) and AlexaFluor-647 (A)), has a calculated R_0 value of 51 Å, assuming $\kappa^2 = 2/3$. For TATA DNAs containing these two fluorophores (one on each 3′ end), three fluorescence measurements were made using a Typhoon fluorimager: (1) fluorescence of the donor (D) fluorophore, (2) fluorescence of the acceptor fluorophore (A), and (3) FRET (F), which was observed by exciting D and measuring emission from A. Laser and filter settings were applied as follows: D, 532 nm excitation/580 nm with 20 nm bandpass emission; A, 633 nm excitation/670 nm with 30 nm bandpass emission; and F, 532 nm excitation/670 nm with 30 nm bandpass emission. The FRET efficiency can be calculated from:

$$E = (F_{\text{corr}})/(F_{\text{corr}} + D_{\text{corr}})$$

The following discussion explains how D_{corr} and F_{corr} were determined. When measuring FRET, extra signal can be observed due to donor bleed-through and acceptor direct excitation. To correct for these spectral overlaps, χ_D and χ_A were determined using TATA DNAs labeled with only a single fluorophore. χ_D was determined by using a donor-only DNA excited at 532 nm with emissions collected at 580 nm (D) and 670 nm (F), where:

$$\chi_D = (F/D)_{(\text{D only})}$$

χ_A was calculated by using an acceptor-only DNA excited at 532 nm (F) or 630 nm (A) with emission collected at 670 nm, where:

$$\chi_A = (F/D)_{(\text{A only})}$$

Spectral overlap for χ_D and χ_A were 0.065 and 0.042, respectively. These values, which are based on the excitation and emission properties of the two fluorophores and the instrument used, remained constant throughout the experiments using the Typhoon fluorimager. Overlap-corrected FRET (F^*) was calculated using:

$$F^* = F - (\chi_D D) - (\chi_A A)$$

When binding protein to fluorescent constructs, potential changes in fluorescence intensity may occur due to changes in the local environments of the fluorophores. Changes in fluorescence intensity between unbound and bound species were determined for both the donor (σ_D) and acceptor (σ_A) fluorophores. σ_D was calculated by dividing the donor signal of bound DNA (b) by donor signal of unbound DNA (u) using a donor only labeled construct:

$$\sigma_D = D_b/D_u$$

σ_A was calculated by dividing the acceptor signal of bound DNA by the acceptor signal of unbound DNA in a D-A pair:

$$\sigma_A = A_b/A_u$$

Acceptor only constructs were not needed, because the acceptor signal remains the same regardless of the degree of FRET (data not shown). Donor and FRET signals were corrected using the following:

$$F_{\text{corr}} = F^*/\sigma_A$$

$$D_{\text{corr}} = D/\sigma_D$$

When performing gelFRET, the amount of DNA probe in the unbound and bound states was not typically the same due to loading differences, non-saturating binding conditions, and/or complex decay; therefore, calculations for fluorescence intensity could not be performed in the manner used for solution based assays. To account for fluorescence intensity changes in gels, an internal control was used that consisted of either a donor only construct containing a (5′- ^{32}P) on the strand with the donor fluorophore or a D-A pair containing a (5′- ^{32}P) on the strand with the acceptor fluorophore. The fluorescence signals of unbound and bound species were then divided by the phosphorimager signal (P) to normalize for the amount of DNA present, where:

$$\sigma_D = (D/P)_b/(D/P)_u$$

$$\sigma_A = (A/P)_b/(A/P)_u$$

Measurement of dissociation rate constants

Reactions were assembled as described earlier and contained 5 nM TATA DNA, 19 nM TBP, and 38 nM TFIIA, where indicated. Complexes were allowed to form for 20 min at room temperature. Dissociation was measured over time after the addition of unlabeled TATA-14 to a final concentration of 1–4 μM; the dissociation rate constants for TBP/TATA-14 complexes measured at 50 mM KCl and 140 mM KCl were unaffected by competitor concentration over this range. Experiments were performed using a Fluorolog-3™ fluorimeter (Yvon/Horiba), DataMax™ Software, and a 12 μl cuvette (Nova Biotech). Fluorescence was measured by exciting at 532 nm and collecting emission at 580 nm (5 nm bandpass) and 670 nm (5 nm bandpass) for donor (D) and FRET (F) signals, respectively. Signals were background corrected, and FRET efficiency (E) was calculated by the equation $E = F/(F+D)$. Relative FRET efficiency was plotted *versus* time in seconds and data were fit with the equation $E = (E_{\text{bound}} - E_{\text{unbound}})e^{(-kt)} + E_{\text{unbound}}$ using Prism® software to

solve for k. The plots shown were normalized by the equation $y=(E-E_{unbound})/(E_{bound}-E_{unbound})$. Physiological salt concentrations consisted of 140 mM KCl, 5 mM $MgCl_2$, and 5 mM NaCl.

Bend angle calculations using a two-kink model

To relate distance changes to a conformational change within the DNA template upon TBP binding, we calculated a DNA bend angle (α) using a modified version of the two-kink model (Figure 2(c)) derived by Parkhurst and colleagues, which is based on a crystal structure of yeast TBP bound to TATA DNA.[19] The model has also been applied to human TBP/TATA complexes.[18] The two-kink model uses the end-to-end distances of the unbound DNA (R_u, Å) and the TBP-bound DNA (R_b, Å) to calculate a DNA bend angle. The DNA molecule is treated as a rigid rod with three segments, of length L_1, L_2, and L_3, and two "hinges" that separate the three segments (see Figure 2(c)). Two bends of exterior angle θ occur at the two hinges. Therefore the total bend angle is $\alpha=2\theta$. In the original model, the TATA box was positioned in the center of the DNA constructs used for the FRET studies, thereby making L_1 equal to L_3.[19] L_2 was determined to be 20.4 Å.[19] In our constructs, L_2 was also 20.4 Å, but the TATA box was not centered. It was offset by the addition of an extra base-pair to L_1 and the removal of one base-pair from L_3. L_1 and L_3 were calculated from R_u using the following:

$$L_1 = (R_u - L_2)/2 + 3.4$$

$$L_3 = (R_u - L_2)/2 - 3.4$$

The left end of the construct lies at the origin of a coordinate system, and all three segments lie in the xy plane (see Figure 2(c)). The position of the right end of the construct is therefore at the x, y coordinates:

$$x = L_1\cos\theta + L_2 + L_3\cos\theta$$

$$y = L_1\sin\theta - L_3\sin\theta$$

The total end-to-end distance of the molecule is R_b, which is given by:

$$R_b^2 = x^2 + y^2$$

Two-kink-twist model

To generate the two-kink-twist model, a twist of angle γ was allowed to occur at the second hinge, between the second and third segments. (Note that no loss of generality occurs in assuming that all the twist occurs between segment 1 and segment 2: we can always choose the coordinates such that these segments are in the same plane.) In the coordinate system (see Figure 7(b)), the left end of segment 1 lies at the origin, segment 1 and segment 2 lie in the xy plane, and the twist moves the right end of segment 3 in the z direction, out of the xy plane. In this system, γ is the angle between the projection of the end of the segment 3 in the yz plane and the negative y axis.

The right end of segment 3 is at position ($L_1\cos\theta$, $-L_2\sin\theta\cos\gamma$, $L_3\sin\theta\sin\gamma$) relative to the right end of segment 2. The position of the right end of the molecule is therefore at the x, y, z coordinates:

$$x = L_1\cos\theta + L_2 + L_3\cos\theta$$

$$y = L_1\sin\theta - L_2\sin\theta\cos\gamma$$

$$z = L_3\sin\theta\sin\gamma$$

The total end-to-end distance of the molecule is R_b, which is given by:

$$R_b^2 = x^2 + y^2 + z^2$$

L_2=20.4 Å and the lengths L_1 and L_3 were calculated as described in the previous section.

Acknowledgements

This research was supported by grant PHY-0404286 from the National Science Foundation and an award from the Butcher Foundation. A.R.H. was supported in part by NIH predoctoral training grant T32 GM065103. T.T.P. is a member of NIST's quantum physics division. Mention of commercial products does not imply NIST recommendation, endorsement, nor that NIST believes these products are the best available for the purpose.

References

1. Pugh, B. F. (2000). Control of gene expression through regulation of the TATA-binding protein. *Gene*, **255**, 1–14.
2. Smale, S. T. & Kadonaga, J. T. (2003). The RNA polymerase II core promoter. *Annu. Rev. Biochem.* **72**, 449–479.
3. Thomas, M. C. & Chiang, C. M. (2006). The general transcription machinery and general cofactors. *Crit. Rev. Biochem. Mol. Biol.* **41**, 105–178.
4. Starr, D. B. & Hawley, D. K. (1991). TFIID binds the minor groove of the TATA box. *Cell*, **67**, 1231–1240.
5. Lee, D. K., Horikoshi, M. & Roeder, R. G. (1991). Interaction of TFIID in the minor groove of the TATA element. *Cell*, **67**, 1241–1250.
6. Horikoshi, M., Bertuccioli, R., Takada, R., Wang, J., Yamamoto, T. & Roeder, R. (1992). Transcription factor TFIID induces DNA bending upon binding to the TATA element. *Proc. Natl Acad. Sci. USA*, **89**, 1060–1064.
7. Starr, D. B., Hoopes, B. C. & Hawley, D. K. (1995). DNA bending is an important component of site-specific recognition by the TATA binding protein. *J. Mol. Biol.* **250**, 434–446.
8. Juo, Z. S., Chiu, T. K., Leiberman, P. M., Baikalov, I., Berk, A. J. & Dickerson, R. E. (1996). How proteins recognize the TATA box. *J. Mol. Biol.* **261**, 239–254.
9. Kim, Y., Geiger, J. H., Hahn, S. & Sigler, P. B. (1993). Crystal structure of a yeast TBP/TATA-box complex. *Nature*, **365**, 512–520.

10. Kim, J. L., Nikolov, D. B. & Burley, S. K. (1993). Co-crystal structure of TBP recognizing the minor groove of a TATA element. *Nature*, **365**, 520–527.
11. Nikolov, D. B., Chen, H., Halay, E. D., Hoffman, A., Roeder, R. G. & Burley, S. K. (1996). Crystal structure of a human TATA box-binding protein/TATA element complex. *Proc. Natl Acad. Sci. USA*, **93**, 4862–4867.
12. Qian, X., Strahs, D. & Schlick, T. (2001). Dynamic simulations of 13 TATA variants refine kinetic hypotheses of sequence/activity relationships. *J. Mol. Biol.* **308**, 681–703.
13. Strahs, D., Barash, D., Qian, X. & Schlick, T. (2003). Sequence-dependent solution structure and motions of 13 TATA/TBP (TATA-box binding protein) complexes. *Biopolymers*, **69**, 216–243.
14. Parvin, J. D., McCormick, R. J., Sharp, P. A. & Fisher, D. E. (1995). Pre-bending of a promoter sequence enhances affinity for the TATA-binding factor. *Nature*, **373**, 724–727.
15. Bareket-Samish, A., Cohen, I. & Haran, T. E. (2000). Signals for TBP/TATA box recognition. *J. Mol. Biol.* **299**, 965–977.
16. Grove, A., Galeone, A., Yu, E., Mayol, L. & Geiduschek, E. P. (1998). Affinity, stability and polarity of binding of the TATA binding protein governed by flexure at the TATA Box. *J. Mol. Biol.* **282**, 731–739.
17. Parkhurst, K. M., Brenowitz, M. & Parkhurst, L. J. (1996). Simultaneous binding and bending of promoter DNA by the TATA binding protein: real time kinetic measurements. *Biochemistry*, **35**, 7459–7465.
18. Masters, K. M., Parkhurst, K. M., Daugherty, M. A. & Parkhurst, L. J. (2003). Native human TATA-binding protein simultaneously binds and bends promoter DNA without a slow isomerization step or TFIIB requirement. *J. Biol. Chem.* **278**, 31685–31690.
19. Wu, J., Parkhurst, K. M., Powell, R. M., Brenowitz, M. & Parkhurst, L. J. (2001). DNA bends in TATA-binding protein-TATA complexes in solution are DNA sequence-dependent. *J. Biol. Chem.* **276**, 14614–14622.
20. Powell, R. M., Parkhurst, K. M., Brenowitz, M. & Parkhurst, L. J. (2001). Marked stepwise differences within a common kinetic mechanism characterize TATA-binding protein interactions with two consensus promoters. *J. Biol. Chem.* **276**, 29782–29791.
21. Petri, V., Hsieh, M., Jamison, E. & Brenowitz, M. (1998). DNA sequence-specific recognition by the *Saccharomyces cerevisiae* "TATA" binding protein: promoter-dependent differences in the thermodynamics and kinetics of binding. *Biochemistry*, **37**, 15842–15849.
22. O'Brien, R., DeDecker, B., Fleming, K. G., Sigler, P. B. & Ladbury, J. E. (1998). The effects of salt on the TATA binding protein-DNA interaction from a hyperthermophilic archaeon. *J. Mol. Biol.* **279**, 117–125.
23. Bergqvist, S., O'Brien, R. & Ladbury, J. E. (2001). Site-specific cation binding mediates TATA binding protein-DNA interaction from a hyperthermophilic archaeon. *Biochemistry*, **40**, 2419–2425.
24. Peterson, M. G., Tanese, N., Pugh, B. F. & Tjian, R. (1990). Functional domains and upstream activation properties of cloned human TATA binding protein. *Science*, **248**, 1625–1630.
25. Weideman, C. A., Netter, R. C., Benjamin, L. R., McAllister, J. J., Schmiedekamp, L. A., Coleman, R. A. & Pugh, B. F. (1997). Dynamic interplay of TFIIA, TBP and TATA DNA. *J. Mol. Biol.* **271**, 61–75.
26. Yokomori, K., Zeidler, M. P., Chen, J.-L., Verrijzer, C. P., Mlodzik, M. & Tjian, R. (1994). Drosophila TFIIA directs cooperative DNA binding with TBP and mediates transcriptional activation. *Genes Dev.* **8**, 2313–2323.
27. DeJong, J. & Roeder, R. G. (1993). A single cDNA, hTFIIA/alpha, encodes both the p35 and p19 subunits of human TFIIA. *Genes Dev.* **7**, 2220–2234.
28. Ma, D., Watanabe, H., Mermelstein, F., Admon, A., Oguri, K., Sun, X. *et al.* (1993). Isolation of a cDNA encoding the largest subunit of TFIIA reveals functions important for activated transcription. *Genes Dev.* **7**, 2246–2257.
29. Ozer, J., Moore, P. A., Bolden, A. H., Lee, A., Rosen, C. A. & Lieberman, P. M. (1994). Molecular cloning of the small (gamma) subunit of human TFIIA reveals functions critical for activated transcription. *Genes Dev.* **8**, 2324–2335.
30. Sun, X., Ma, D., Sheldon, M., Yeung, K. & Reinberg, D. (1994). Reconstitution of human TFIIA activity from recombinant polypeptides: a role in TFIID-mediated transcription. *Genes Dev.* **8**, 2336–2348.
31. Bleichenbacher, M., Tan, S. & Richmond, T. J. (2003). Novel interactions between the components of human and yeast TFIIA/TBP/DNA complexes. *J. Mol. Biol.* **332**, 783–793.
32. Langelier, M. F., Forget, D., Rojas, A., Porlier, Y., Burton, Z. F. & Coulombe, B. (2001). Structural and functional interactions of transcription factor (TF) IIA with TFIIE and TFIIF in transcription initiation by RNA polymerase II. *J. Biol. Chem.* **276**, 38652–38657.
33. Lieberman, P. M., Ozer, J. & Gursel, D. B. (1997). Requirement for transcription factor IIA (TFIIA)-TFIID recruitment by an activator depends on promoter structure and template competition. *Mol. Cell. Biol.* **17**, 6624–6632.
34. Lagrange, T., Kim, T. K., Orphanides, G., Ebright, Y. W., Ebright, R. H. & Reinberg, D. (1996). High-resolution mapping of nucleoprotein complexes by site-specific protein-DNA photocrosslinking: organization of the human TBP-TFIIA-TFIIB-DNA quaternary complex. *Proc. Natl Acad. Sci. USA*, **93**, 10620–10625.
35. Tan, S., Hunziker, Y., Sargent, D. F. & Richmond, T. J. (1996). Crystal structure of a yeast TFIIA/TBP/DNA complex. *Nature*, **381**, 127–134.
36. Geiger, J. H., Hahn, S., Lee, S. & Sigler, P. B. (1996). Crystal structure of the yeast TFIIA/TBP/DNA complex. *Science*, **272**, 830–836.
37. Ramirez-Carrozzi, V. & Kerppola, T. (2001). Gel-based fluorescence resonance energy transfer (gel-FRET) analysis of nucleoprotein complex architecture. *Methods*, **25**, 31–43.
38. Bernues, J., Carrera, P. & Azorin, F. (1996). TBP binds the transcriptionally inactive TA5 sequence but the resulting complex is not efficiently recognised by TFIIB and TFIIA. *Nucl. Acids Res.* **24**, 2950–2958.
39. Wu, S. Y. & Chiang, C. M. (2001). TATA-binding protein-associated factors enhance the recruitment of RNA polymerase II by transcriptional activators. *J. Biol. Chem.* **276**, 34235–34243.
40. Wobbe, C. R. & Struhl, K. (1990). Yeast and human TATA-binding proteins have nearly identical DNA sequence requirements for transcription *in vitro*. *Mol. Cell. Biol.* **10**, 3859–3867.
41. Parkhurst, K. M., Richards, R. M., Brenowitz, M. & Parkhurst, L. J. (1999). Intermediate species possessing bent DNA are present along the pathway to formation of a final TBP-TATA complex. *J. Mol. Biol.* **289**, 1327–1341.

42. Hoopes, B. C., LeBlanc, J. F. & Hawley, D. K. (1998). Contributions of the TATA box sequence to rate-limiting steps in transcription initiation by RNA polymerase II. *J. Mol. Biol.* **277**, 1015–1031.
43. Galasinski, S. K., Lively, T. N., Grebe de Barron, A. & Goodrich, J. A. (2000). Acetyl-CoA stimulates RNA polymerase II transcription and promoter binding by TFIID in the absence of histones. *Mol. Cell. Biol.* **20**, 1923–1930.
44. Weaver, J. R., Kugel, J. F. & Goodrich, J. A. (2005). The sequence at specific positions in the early transcribed region sets the rate of transcript synthesis by RNA polymerase II *in vitro*. *J. Biol. Chem.* **280**, 39860–39869.
45. Hillisch, A., Lorenz, M. & Diekmann, S. (2001). Recent advances in FRET: distance determination in protein-DNA complexes. *Curr. Opin. Struct. Biol.* **11**, 201–207.

Edited by J. O. Thomas

(Received 26 March 2007; received in revised form 11 June 2007; accepted 25 June 2007)
Available online 29 June 2007